

GROUND SOURCE HEAT PUMP MODELLING WITH THERMAL STORAGE – SIMULATION AND INTEGRATION ISSUES IN ENERGYPLUS

Aidan T. Jones, Donal P. Finn
School of Mechanical and Materials Engineering
University College Dublin, Ireland

ABSTRACT

This paper describes the modelling of two major system components as part of a retrofit installation of a thermally massive building, where a ground source heat pump and a phase change thermal energy storage system are installed. The two models are presented, as is their incorporation into the EnergyPlus whole building simulation program, used to model the building fabric and other system components. A model of the high temperature thermal storage unit, consisting of phase change material encapsulated in flat plates, is described. The model, which uses a first order finite difference method, is defined in Matlab and connected as a plant component in EnergyPlus through the Building Controls Virtual Test Bed. The effect of changing the heat transfer fluid (water) mass flow rate on the rate of charging is presented. A model of a building-integrated ground source heat pump is also described. It is represented in EnergyPlus using the Energy Management System user-defined plant component object. This paper presents a novel approach to modelling these components together in the same EnergyPlus simulation.

INTRODUCTION

Concerns about the continued sustainability of fossil fuel resources, from both economic and security perspectives, has led to increased interest in non-fossil fuel resources, particularly renewable energy systems (RES). This transition has been quite evident in certain national or regional electricity grids, where increasing proportions of power comes from renewable resources, a case in point being wind in Ireland (SEAI 2010). For some grid systems, wind can, at certain times and under particular conditions, constitute a significant fraction of the overall supply. Coupled with these developments, is an increased interest in the electrification of heating and cooling loads within buildings. In this context, Ground Source Heat Pumps (GSHPs) offer an attractive, electrically-driven means of meeting building heating and cooling loads. Moreover, as buildings constitute a large proportion of electricity demand, the demand flexibility offered heating and cooling loads will become increasingly important. Such demand

flexibility is necessary particularly for electricity grids where wind generation, which is variable in nature, constitutes a significant contribution to the generation mix (Moura & de Almeida 2010).

In such situations, integrated building thermal energy storage (TES) offers the potential of shifting building electricity consumption from peak to off-peak times or if aggregated sufficiently across the grid, where supply-demand mismatches occur. Given that in 2010, 33.5% of electricity in US buildings was used for space heating and cooling and water heating (US DOE 2011), the potential of load shifting from increased thermal load flexibility is significant. Storage in the form of large active systems, either as water calorifiers or hydronic integrated phase change materials capsules, is of increasing interest in many building retrofit projects. Retrofit projects also exhibit additional opportunities and challenges associated with passive thermal energy storage characteristics arising from building fabric itself, especially in the case of thermally massive buildings (Braun 1990). In such retrofit scenarios, the use and control of active thermal energy storage, in conjunction with passive energy storage behaviour in buildings adds increased possibilities and complexity.

Control of active TES systems is essential if the benefits of added flexibility brought about by such technology are to be fully exploited.

LITERATURE REVIEW

Modelling of phase change material (PCM) TES systems has seen significant attention in the literature. Elsayed (2007) describes charging of a PCM tank consisting of flat encapsulated plates subject to cyclic temperature conditions. Simulation predictions were validated against experimental data from Chang-Yong & Hsieh (1992) and showed that the heat transfer fluid (HTF) temperature had a greater effect on the heat stored, compared to the pumping regime used during charging and discharging of the TES units. Liu et al. (2011) describes a one-dimensional finite difference model of a TES unit consisting of PCM encapsulated flat plates. Comparison of the modelled results against experimental data shows good agreement for TES

outlet heat transfer fluid temperatures as well as heat transfer profiles. D'Avignon & Kummert (2012) developed a flat plate PCM TSU model based on the enthalpy method, with phase change taking place over a small temperature range. The model, which was integrated with TRNSYS, was validated using data from Liu et al. (2011) and showed that errors were larger with increased time step and node length. Wei et al. (2005) examined the heat release characteristics of four PCM encapsulation shapes: spheres, cylinders, flat plates and tubes, showing spheres to have the best heat release characteristics. A constant PCM melting temperature was assumed, while taking into account the effect of freezing PCM within the capsules.

Ihm et al. (2004) incorporated a PCM TES model into EnergyPlus as the *ThermalStorage* objects, based on an ice storage model by Taylor et al. (1993), for use within the BLAST simulation program. Results of a case study showed that the location of the tank (upstream, downstream or parallel to the chiller) was unimportant to the simulation results. Halawa et al. (2010) developed a one dimensional algorithm for representing phase change processes.

In several instances of the literature, the benefits of combined active and passive storage are discussed. A simulation environment is described (Hajiah & Krarti 2012a, 2012b), indicating that a saving of up to 28% on cooling costs can be achieved through optimising both precooling and active thermal storage and found that savings increased with increased ice tank size. Other studies show that predictive optimal control of active and passive storage can be used to reduce energy costs in a time-of-use framework (Henze 2005). Henze & Krarti (2003) analysed the use of the combination of active and passive storage using EnergyPlus.

In order to develop building integrated control algorithms for integration and optimisation of active TES systems in building retrofit programmes, modelling of the entire building integrated system is essential. In this paper, models of a thermal storage unit (TSU), consisting of phase change material encapsulated in flat plates, and a GSHP are described, as well as their incorporation into the EnergyPlus whole building simulation program.

SIMULATION METHODOLOGY

Building and HVAC Plant

The main simulation program used in this research paper is EnergyPlus. The building under consideration is a municipal building in Coimbra, Portugal. It is being used as a GroundMed demonstration site under the auspices of the University of Coimbra. The building is a municipal office block with walls, constructed of solid limestone, up to 69 cm thick. A retrofit GSHP that meets both the heating and cooling loads of the third

floor of the building was installed. There are 33 air coil units distributed in 20 conditioned zones on the third floor of the building.

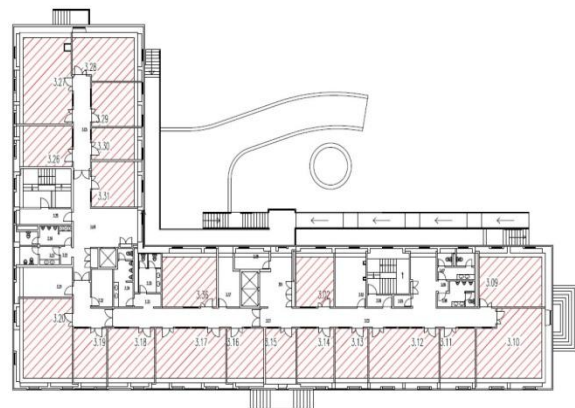


Figure 1: Plan view of third floor

As shown in Figure 2, the building integrated heat pump circuit is composed of a ground loop and two building loops, each with their own variable speed pumps. The ground loop contains the ground heat exchanger (GHE), consisting of seven vertical parallel double u-tubes and is modelled using the inbuilt EnergyPlus *GroundHeatExchanger* object. The building hydronic circuit consists of a primary loop, incorporating the GSHP and TES unit and a secondary loop incorporating the zone fan coils. A decoupling tank separates the primary from the secondary loop.

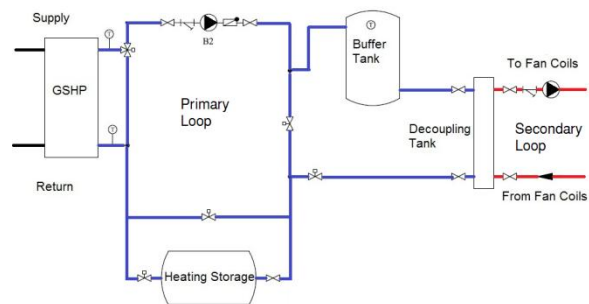


Figure 2: Plant Circuit Layout

Ground Source Heat Pump Model

The GSHP is modelled within EnergyPlus. Two existing ground source heat pump modelling approaches were considered: a parametric model (Jin 2002) and an equation-fit based model (Tang 2005). The parametric model, which is based on a physical modelling approach, requires considerable detail about the physical specifications of the heat pump and was not considered further in this work. The equation-fit model uses equations of the form shown in Equation 1 to obtain heating and cooling capacity, as well as power consumption of the GSHP.

$$\dot{Q} = C_1 + C_2 \frac{V_L}{V_{ref}} + C_3 \frac{V_S}{V_{ref}} + C_4 \frac{T_L}{T_{ref}} + C_5 \frac{T_S}{T_{ref}} \quad (1)$$

where C_{1-5} are constants, subscripts L and S refer to load and source side respectively and ref denotes reference conditions, while V is volumetric flow rate and T is temperature.

As can be seen from Equation 1, this model relies on linear relationships with flow rates and temperatures to calculate heat pump capacity and power. Equations proposed by Corberan et al. (2011), however, describe a GSHP using quadratic relationships for temperature and mass flow rate. The form of the equation used, for example to describe the heating capacity, is shown in Equation 2, with the result shown graphically in Figure 3(a) and compared to the output from the linear relationship got from Equation 1, Figure 3(b).

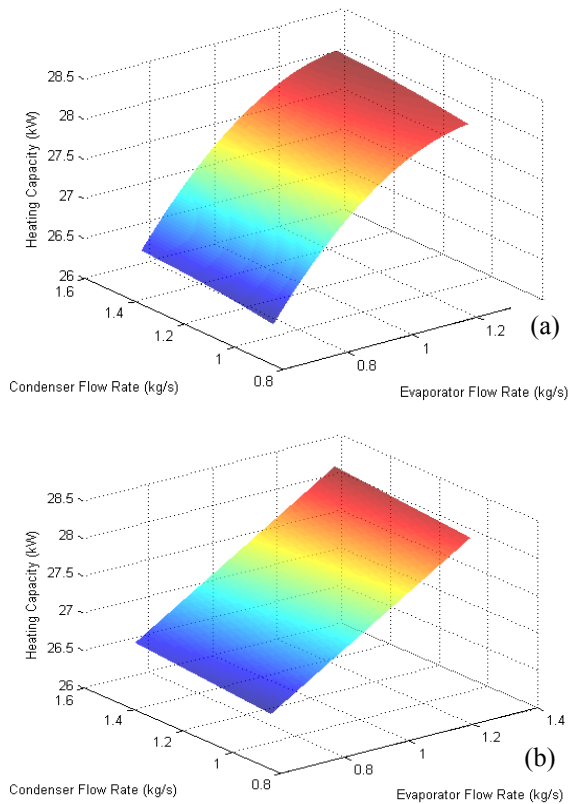


Figure 3: GSHP Heating Capacity for different evaporator and condenser water flow rates for (a) quadratic equations and (b) linear equations

$$\dot{Q}_{heating} = C_1 + C_2 \dot{m}_S + C_3 \dot{m}_S^2 + C_4 \dot{m}_L + C_5 \dot{m}_L^2 + C_6 T_{in,L} + C_7 T_{in,L}^2 + C_8 T_{in,L}/T_{in,S} \quad (2)$$

Equation 2 is used to calculate the heat transfer on the building side in heating mode, where C_{1-7} are

constants and L and S denote the side of the heat pump in question (load and source side respectively). The plots shown are based on data from a GSHP similar to that installed on-site. Characterisation of the GSHP installed at the Coimbra site is ongoing, via in-situ testing and specialised simulation software.

To implement a GSHP based on quadratic equations, instead of the linear relationships provided in the standard EnergyPlus GSHP object, a new user-defined object had to be created. For Energy Plus releases up to Version 7.1, there existed no possibility to create user-defined, equation-based components, without defining a new module through modification and recompilation of the source code.

In version 7.1 of EnergyPlus, the object *PlantComponent:UserDefined* was introduced, facilitating the inclusion of user-defined plant components. These components are described using the Energy Management System (EMS); its operation described in Figure 4. Before execution of EnergyPlus, the *PlantComponent:UserDefined* object sets up the component connections to the plant loop(s). When EnergyPlus is executed, the program calling manager activates two programs: one to initialise the component, the other simulates the component operation. These programs are written in the EnergyPlus runtime language (Erl). Input and output of the programs are defined using EMS *actuator* and *internal variable* objects.

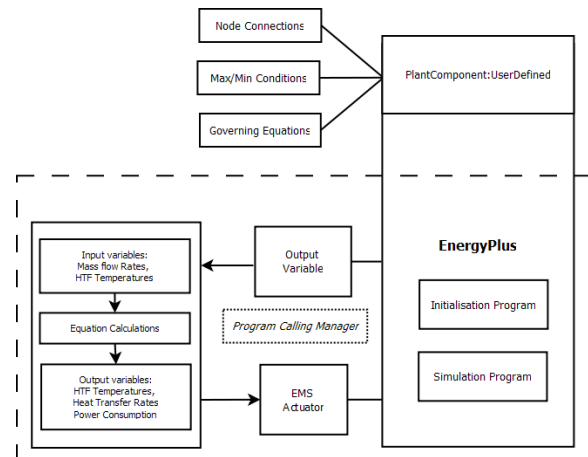


Figure 4: Flow chart describing user-defined plant component operation in EnergyPlus

In the case of the GSHP presented, two plant connections are described: one on the primary plant loop and one on the ground loop. The EMS simulation program reads in the fluid properties on the ground and building sides of the heat pump, as well as the fluid temperatures and mass flow rates. On each side of the GSHP, three equations are used (such as Equation 2) to calculate:

- i. heat transfer on the building side
- ii. heat transfer on the ground side
- iii. power consumed by the compressor

The outlet fluid temperatures are calculated by applying an energy balance across the heat exchangers. Component (condenser, evaporator, compressor) dependent variables (heat transfer, power) are calculated outputted via the EMS and reported in EnergyPlus.

Thermal Storage Model

The retrofit installation at the test site includes a 3m³ heating TSU, with 100kWh capacity. A proposed model is described in this section, outlined in Table 1; the arrangement of the PCM capsules is similar to Figure 5.

Table 1:
PCM tank properties

PCM	Salt Hydrate
Melting Temperature (°C)	46
C _p (kJ/kgK)	2.41
Heat of Fusion (kJ/kg)	190
Thermal Conductivity (W/mK)	0.45
Density (kg/m ³)	1.587
Tank Length (m)	3.5
Tank height = tank width (m)	0.75
Water volume (%)	40

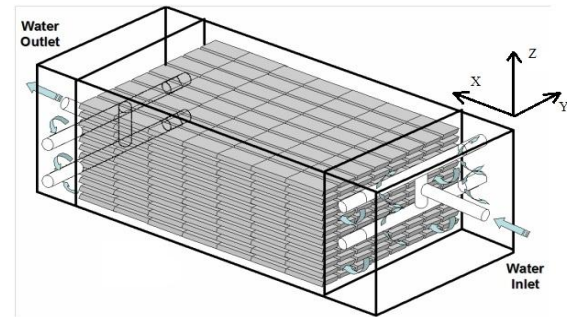


Figure 5: PCM tank arrangement (PCM 2011)

Existing EnergyPlus TSU Model

EnergyPlus has an inbuilt object to model PCM thermal storage; it is based on the work by Ihm et al. (2004). This was deemed unsuitable for this work for the following reasons: (i) the user supplies one charging and one discharging curve, which is insufficient to fully capture the behaviour of the tank (ii) there was no provision for a tank incorporating high temperature energy storage, which is required within this study, (iii) the presence of a GSHP object on the same plant loop was incompatible with the use of the PCM TSU object: the setpoint of the GSHP could not be set independently of the TSU, leaving the user no control of the TSU when using a GSHP. The EMS user-defined plant component object does not have the capabilities to produce a finite difference model, meaning that within the confines of EnergyPlus, there was no possibility of completing the desired model in a satisfactory manner.

Proposed Finite Difference Model

A forward finite difference model was developed in Matlab to simulate the charging and discharging of the active thermal storage unit. The model assumed a fixed PCM melting temperature, with no supercooling; constant HTF properties; no external losses and one-dimensional heat transfer. The tank is divided into contiguous control volumes (nodes) of equal length. The width and height of each node is the equal to those of the tank.

Heat transfer regime

A thermal resistance network is used to define heat transfer within each control volume. Heat transfer (Q [J]) is calculated for each control volume and time step using the following equations:

$$Q = (T_{HTF} - T_{PCM}) * timestep / R_{Total} \quad (3)$$

$$R_{Total} = R_{conv} + R_{cond,capsule} + R_{cond,PCM} \quad (4)$$

Where R_{Total} is the sum of the convective and conductive resistances, T_{HTF} and T_{PCM} are the temperatures of the HTF and PCM respectively.

Velraj et al. (1997) noted that the conduction term within a PCM container becomes increasingly important as the liquid/solid PCM front moves from the surface to the interior of the vessel. Within the model, this is taken into account by inclusion of conduction resistance term ($R_{conv,PCM}$) within each PCM slab. Within each control volume, this PCM resistance term will be different, depending on the liquid fraction and is defined as follows:

$$R_{cond,PCM} = \frac{t_{PCM}}{k_{PCM}A} \quad (5)$$

where k_{PCM} is the conductivity of the PCM resisting heat transfer, t_{PCM} is distance of the solid/liquid front from the capsule surface and A is the surface area of the capsule.

The HTF convection resistance term is based on a Nusselt number (Nu) correlation,

$$R_{conv} = D_h / Nu \cdot k_{water} \cdot A \quad (6)$$

Where D_h is the hydraulic diameter. A laminar flow regime is assumed at all points within the tank. Hence, Nu is calculated by Equation 7 (Shah & London 1978):

$$Nu_{x,T} = \begin{cases} 1.233(x^*)^{-\frac{1}{3}} + 0.4, & x^* \leq 0.001 \\ 7.541 + 6.874(10^3 x^*)^{-0.488} e^{-2.45x^*}, & x^* < 0.001 \end{cases} \quad (7)$$

Where $x^* = \left(\frac{x}{D_h}\right) / (Re \cdot Pr)$, x is distance from the inlet, Re Reynolds number and Pr is Prandtl number.

Heat Balance

Through performance of a heat balance at each node, the HTF outlet temperature, PCM temperature and liquid fraction for the next time step are calculated using a series of equations; some examples are given in given in Table 2 for charging mode.

*Table 2:
Equations for PCM and liquid fraction when charging the heating storage*

$T_{PCM} < T_{melt}$	$T_{PCM}^{i+1} = T_{PCM}^i + \frac{Q^i}{C_{p,PCM,solid} m_{PCM,node}}$
	$X^{i+1} = X^i$
$T_{PCM} = T_{melt}$	$T_{PCM}^{i+1} = T_{PCM}^i$
	$X^{i+1} = X^i + \frac{Q^i}{l_{PCM} m_{PCM,node}}$
$T_{PCM} > T_{melt}$	$T_{PCM}^{i+1} = T_{PCM}^i + \frac{Q^i}{C_{p,PCM,liquid} m_{PCM,node}}$
	$X^{i+1} = X^i$

where $C_{p,PCM,solid}$ and $C_{p,PCM,liquid}$ refer to the specific heat capacities of the PCM in solid and liquid state. l_{PCM} is the latent heat of fusion of the PCM, $m_{node,PCM}$ is the mass of PCM in a control volume, X is the liquid fraction, T_{melt} is the melting temperature of the PCM and i refers to the time step.

To use the Matlab model as a component in EnergyPlus, it must be connected through an external interface: Ptolemy and the Building Controls Virtual Test Bed (BCVTB).

Building Controls Virtual Test Bed

Building Controls Virtual Test Bed (BCVTB) allows Matlab to access the External Interface objects in EnergyPlus, which act exactly as EMS objects. In a similar manner to the GSHP above, a TSU component is declared with the user-defined component object, but the component outlet temperature is calculated by the Matlab program and overwrites that from the EMS program. BCVTB calls both EnergyPlus and Matlab at each time step, during which there is a data exchange between the two programs. EnergyPlus outputs the TSU inlet conditions. Matlab executes the TSU model and outputs the HTF outlet temperature, along with the state of charge and heat transferred during the time step. These are read into EnergyPlus through the External Interface.

The timestep for the Matlab model must be the same as that for the EnergyPlus. EnergyPlus has a minimum timestep of one minute, which was deemed too long for this TSU model. To manage the different

timesteps between Matlab and EnergyPlus, two timesteps were chosen for use within Matlab – one equal to that in EnergyPlus and one shorter. Each time the Matlab model is called by BCVTB, the TSU model iterates using the smaller internal timestep and at the end of each longer timestep, returns the output variables to BCVTB for use in EnergyPlus.

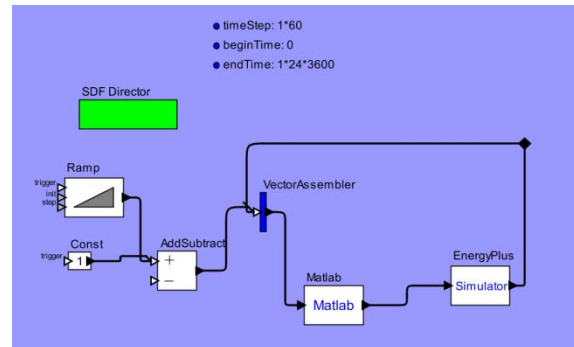


Figure 6: Layout of BCVTB: Matlab, EnergyPlus

RESULTS

The only output EnergyPlus explicitly requires from the Matlab TSU model to continue the simulation is the outlet water temperature. Outlet temperature against time is shown in Figure 7 for charging mode. Initially, the outlet temperature increases quickly to reach the PCM melting temperature (46°C) from the initial temperature of 40°C. As time progresses, the temperature approaches that of the inlet temperature (50°C), as heat transfer decreases to zero (Figure 8).

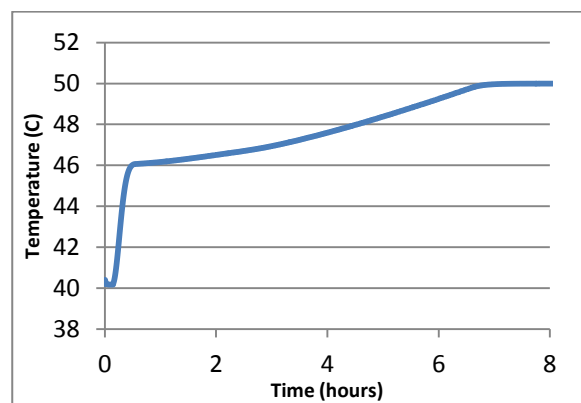


Figure 7: TES Outlet water temperature for inlet temperature of 50°C and a mass flow rate of 1.5 kg/s

Figure 8 shows the effect on the heat transferred by changing mass flow rates. The heat transfer rate increases with increased flow rate and the associated charging time decreases. The overall heat transfer rate reduces to zero as the nodes become fully charges and as the thermal resistance within each capsule due to melting PCM increases.

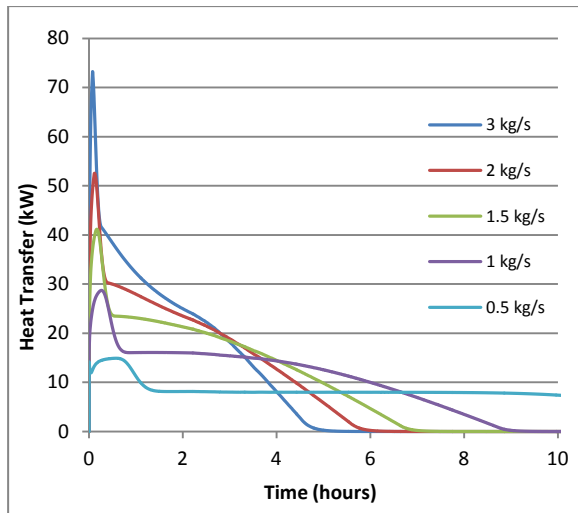


Figure 8: Heat transfer rate vs. time for different HTF flow rates, $T_{in,water} 50^{\circ}C$

Figure 9 shows the HTF temperature distribution across the tank (0 being inlet and 1 being outlet) for increasing time during the charging process. As time progresses, the outlet temperature can be seen to increase. At later times in the process, the temperature of the HTF remains at $50^{\circ}C$ (the inlet temperature) for the first portion of the tank, indicating that it is fully charged up until the point, after which the temperature begins to decrease as heat transfer takes place.

Figure 10 shows a similar plot of state of charge across the tank for different times, with the tank being fully charged at all points within the tank at the end of the charging process. It can be seen that the tank is charged more quickly in the regions close to the entrance, with the state of charge decreasing towards the tank exit. The regions towards the outlet of the tank only become fully charged after the entrance regions have become so.

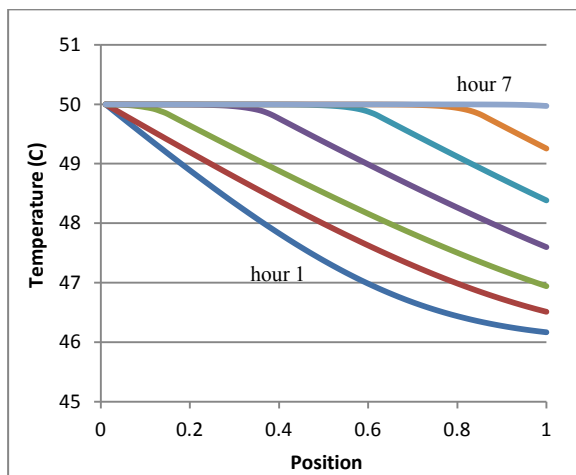


Figure 9: $T_{HTF,out}$ vs. TES position for hourly intervals from 1 to 7 hours, $T_{in,water} 50^{\circ}C$

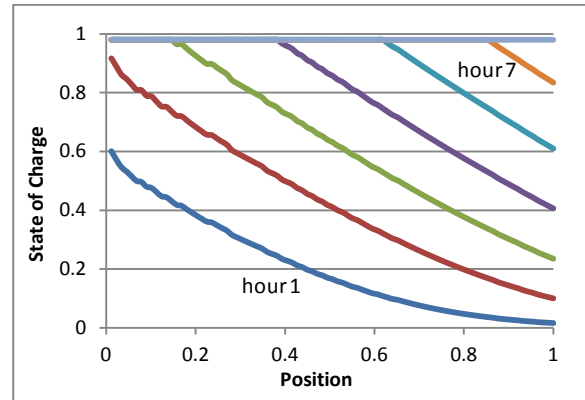


Figure 10: State of charge versus position for hourly intervals between 1 and 7 hours, $T_{in,water} 50^{\circ}C$

From Figure 11, it is interesting to note the difference dynamic nature of charging a TSU within an entire plant system. The presence of the TSU acts as an extra load to the GSHP, leading to longer on cycles. In an isolated model of a TSU, the cycling of the heat source would not be accounted for, nor would the effects of changing building load and external temperatures. The heat transfer rate to the TSU increases with rising GSHP outlet temperature. When the GSHP cycles off, a sharp drop in heat transfer is seen, corresponding to the drop in temperature of the water leaving the heat pump. The gradual decrease in TSU heat transfer is due to the time taken for changes in temperature to propagate through the TSU.

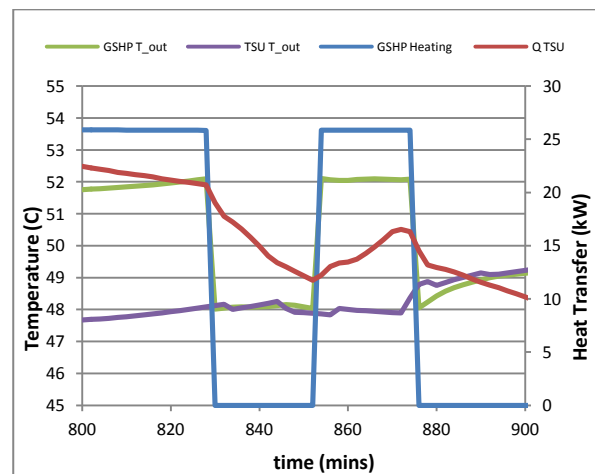


Figure 11: EnergyPlus output showing the effect of HP cycling on TSU and GSHP temperatures

Conclusions

Presented in this paper are comprehensive models of a GSHP and a PCM TSU. The work has focused on how to incorporate these models into EnergyPlus. The use of the EMS user-defined plant component model allows for a more accessible means of modelling a GSHP, with greater possibilities for

control now available. The incorporation of a PCM TSU model which uses a finite difference method is new to EnergyPlus. Demonstrated in this paper is a method to model components in EnergyPlus using an external program such as Matlab.

This research provides a platform for analysing in greater detail the plant interactions of a GSHP and PCM TSU. The ability to use EnergyPlus as a tool to optimise these two components, along with the opportunities presented by passive thermal storage is possible following this work.

NOMENCLATURE

Acronyms

<i>BCVTB</i>	= Building Controls Virtual Test Bed
<i>EMS</i>	= Energy Management System
<i>Erl</i>	= EnergyPlus runtime language
<i>GSHP</i>	= ground source heat pump
<i>GHE</i>	= ground heat exchanger
<i>HTF</i>	= heat transfer fluid
<i>PCM</i>	= phase change material
<i>RES</i>	= renewable energy systems
<i>TES</i>	= thermal energy storage
<i>TSU</i>	= thermal storage unit
<i>TOU</i>	= time-of-use

Greek Symbols

ρ	= density (kg/m)
--------	------------------

Variables

<i>A</i>	= surface area (m ²)
<i>C</i>	= heat capacity (kJ/K)
<i>c_p</i>	= specific heat capacity (kJ/kg·K)
<i>D_h</i>	= hydraulic diameter (m)
<i>k</i>	= thermal conductivity (W/m·K)
<i>l</i>	= latent heat of fusion (kJ/kg)
<i>ṁ</i>	= mass flow rate (kg/s)
<i>Nu</i>	= Nusselt number
<i>Pr</i>	= Prandtl number
<i>Q</i>	= heat transfer (J)
<i>Q̇</i>	= heat transfer rate (W)
<i>R</i>	= thermal resistance (K/W)
<i>Re</i>	= Reynolds number
<i>t</i>	= thickness (m)
<i>T</i>	= temperature (°C)
<i>v</i>	= velocity (m/s)
<i>V</i>	= volumetric flow (m ³ /s)
<i>x</i>	= distance from inlet of TSU (m)
<i>x*</i>	= dimensionless distance from TSU inlet
<i>X</i>	= Liquid fraction

Subscripts

<i>cond,1</i>	= PCM capsule shell conductive resistance
<i>cond,2</i>	= charged PCM conductive resistance

<i>conv</i>	= convective resistance from HTF to PCM
<i>i</i>	= this timestep
<i>i+1</i>	= the next timestep
<i>in</i>	= entry value
<i>L</i>	= load side of GSHP
<i>out</i>	= outlet value
<i>ref</i>	= reference condition
<i>S</i>	= source side of GSHP

ACKNOWLEDGEMENT

This research is funded by the European Union through the GroundMed FP7 project (www.groundmed.eu). The cooperation of those at ISR-University of Coimbra Coimbra is appreciated, in particular Professor Anibal De Almeida.

REFERENCES

- Braun, J.E., 1990. Reducing energy costs and peak electrical demand through optimal control of building thermal mass. *ASHRAE Transactions*, pp.264–273.
- Chang-Yong, C. & Hsieh, C.K., 1992. Solution of Stefan problems imposed with cyclic temperature and flux boundary conditions. *International Journal of Heat and Mass Transfer*, 35(5), pp.1181–1195.
- Corberan, J.M., Finn, D.P., Montagud, C., Murphy, F.T., Edwards, K.C., 2011. A quasi-steady state mathematical model of an integrated ground source heat pump for building space control. *Energy and Buildings*, 43(1), pp.82–92.
- D'Avignon, K. & Kummert, M., 2012. Proposed TRNSYS Model for Storage Tank with Encapsulated Phase Change Materials. In *SimBuild*. Wisconsin: IBPSA.
- Elsayed, A.O., 2007. Numerical study of ice melting inside rectangular capsule under cyclic temperature of heat transfer fluid. *Energy Conversion and Management*, 48(1), pp.124–130.
- Hajiah, A. & Krarti, M., 2012a. Optimal control of building storage systems using both ice storage and thermal mass – Part I: Simulation environment. *Energy Conversion and Management*, 64, pp. 499-508.
- Hajiah, A. & Krarti, M., 2012b. Optimal controls of building storage systems using both ice storage and thermal mass – Part II: Parametric analysis. *Energy Conversion and Management*, 64, pp.509-515.
- Halawa, E., Saman, W. & Bruno, F., 2010. A phase change processor method for solving a one-dimensional phase change problem with convection boundary. *Renewable Energy*, 35(8), pp.1688–1695.

Henze, G.P., 2005. Energy and cost minimal control of active and passive building thermal storage inventory. *Journal of Solar Energy Engineering, Transactions of the ASME*, 127(3), pp.343–351.

Henze, G.P. & Krarti, M., 2003. *Predictive Optimal Control of Active and Passive Building Thermal Storage Inventory*, University of Nebraska - Lincoln.

Ihm, P., Krarti, M. & Henze, G.P., 2004. Development of a thermal energy storage model for EnergyPlus. *Energy and Buildings*, 36(8), pp.807–814.

Jin, H., 2002. *Parametric Estimation Based Models of Water Source Heat Pumps*. Master. Oklahoma, USA: Department of Mechanical and Aerospace Engineering, Oklahoma State University.

Liu, M., Saman, W. & Bruno, F., 2011. Validation of a mathematical model for encapsulated phase change material flat slabs for cooling applications. *Applied Thermal Engineering*, 31(14–15), pp.2340–2347.

Moura, P.S. & de Almeida, A.T., 2010. The role of demand-side management in the grid integration of wind power. *Applied Energy*, 87(8), pp.2581–2588.

PCM, 2011. Plus-Ice, Phase Change Material, Thermal Energy Storage (TES) Design Manual. Available: http://www.pcmproducts.net/files/design_manual.pdf

Russell D. Taylor, Pedersen, C.O. & Lawrie, L., 1993. Simulation of Thermal Storage Systems In An Integrated Building Simulation Program. Available: http://apps1.eere.energy.gov/buildings/energyplus/pdfs/bibliography/thermal_storage_simulation_taylor.pdf.

SEAI, 2010. *Renewable Energy in Ireland - 2010 Update*, Sustainable Energy Authority of Ireland. Available: http://www.seai.ie/Publications/Statistics_Publications/SEI_Renewable_Energy_2010_Update/RE_in_Ire_2010update.pdf.

Shah, R.K. & London, A.L., 1978. *Laminar flow forced convection in ducts: a source book for compact heat exchanger analytical data*, New York: Academic Press.

Tang, C.C., 2005. *Modeling Packaged Heat Pumps in a Quasi-Steady State Energy Simulation Program*. Master of Science. Oklahoma: Department of Mechanical and Aerospace Engineering, Oklahoma State University.

US DOE, 2011. Buildings Energy Data Book. Available: <http://buildingsdatabook.eren.doe.gov/TableView.aspx?table=1.1.4>

Velraj, R., Seeniraj, R.V., Hafner, B., Faber, C., 1997. Experimental analysis and numerical modelling of inward solidification on a finned vertical tube for a latent heat storage unit. *Solar Energy*, 60(5), pp.281–290.

Wei, J., Kawaguchi, Y., Hirano, S., Takeuchi, H., 2005. Study on a PCM heat storage system for rapid heat supply. *Applied Thermal Engineering*, 25(17–18), pp.2903–2920.